Diffusion in Zeolites Containing Mixed Cations

Experimental results are reported for equilibrium adsorption and diffusivities of CH_4, C_2H_6 and CO_2 in type A zeolite containing mixed Na and K cations ranging from 0 to 100% in composition, at two temperatures and 1 atm. Two simple theoretical solutions are given for the diffusivity. One is for diffusion with pore (aperture) blocking using the effective medium approximation, which is readily available from the literature on percolation theory. The other is a kinetic solution derived in this work for cavities containing heterogeneous sites, which is a case where the percolation theory is not applicable. The equilibrium adsorption results show that K^+ has a preference for the aperture (or pore-blocking) sites (site type II), and these results are interpreted by the bond percolation theory. The diffusivity results are successfully interpreted by the pore-blocking theory in zeolites containing less than 25% K^+ and by the kinetic theory for zeolites with higher K^+ contents.

Y. T. Yeh
R. T. Yang
Department of Chemical Engineering
State University of New York at Buffalo
Buffalo, NY 14260

Introduction

Diffusion in porous structures with blocked pores and covered (adsorption/reaction) sites is an important problem encountered in many fields and has been the subject of many recent studies (e.g., Gavalas and Kim, 1981; Theodorou and Wei, 1983; Benzoni and Chang, 1984; Sahimi and Tsotsis, 1985; Mo and Wei, 1986; Burganos and Sotirchos, 1987). The pore structure in zeolite molecular sieves is characterized by a regular network of cavities interconnected by apertures (pores). The cavities contain the adsorption and reaction sites whereas the apertures are accountable for the molecular sieving properties. For a given type of zeolite, the aperture size is dependent on the type of cations contained in the crystal. For example, by exchanging the sodium cations of the 4A zeolite with calcium cations, the effective aperture size is increased from about 4 to 5 Å (5A zeolite). Ion exchange of 4A zeolite with potassium cations reduces the apertures to about 3 Å (3A zeolite). Many zeolites, both synthetic and natural, however, contain mixed cations (Breck, 1974; Barrer, 1978). Mixed-cation zeolites exhibit unique adsorption (Breck et al., 1956) and diffusion properties (Ruthven, 1974), and can be prepared by controlled partial ion exchange. These zeolites are sorbents with tailored kinetic selectivities for kinetic separations, i.e., separations caused by differences in diffusivities (Yang, 1987).

Correspondence concerning this paper should be addressed to R. T. Yang.

This paper presents experimental results of adsorption and diffusion in type A zeolite containing mixed sodium and potassium ions. The equilibrium adsorption data are interpreted by the percolation model, and stochastic results are derived for the diffusivity in zeolites with mixed cations.

Theoretical Considerations

Cations in the zeolite cavities are located on specific sites. The crystal structure and cation locations in type A zeolite are shown in Figure 1. The cations located near an aperture (site II in Figure 1) partially block it. (The term "pore" will be used in place of "aperture" to be consistent with the literature on percolation theory.) Other types of cations are entirely enclosed within the cavity (sites I and III in Figure 1). These two types of cations influence the diffusivity of a given gas molecule by different mechanisms. The former type influences the diffusivity by pore blocking, which is a percolation problem and has been treated as "pore percolation" or "bond percolation." The latter type of cations influences the diffusivity by having different bond strengths between the adsorbed gas molecule and the adsorption sites that are associated with different cations. This is not a percolation problem and will hence be treated kinetically. In the following, a theoretical solution will be given for diffusion in zeolite with pore-blocking cations, and a kinetic solution based on heterogeneous sites will be given for diffusion in zeolite with mixed cations occluded in the cavity.

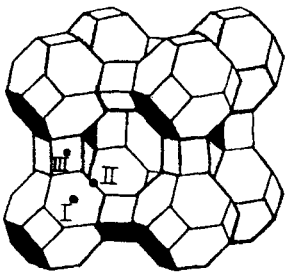

Figure 1. Framework structure of a type A zeolite cavity and three sites where cations are located.

Analytic solutions for pore blocking from effective medium approximation

Numerical solutions for diffusion in 2D or 3D network with blocked or partially-blocked pores can be obtained by Monte Carlo simulation (e.g., Kirkpatrick, 1973; Ruthven, 1974; Theodorou and Wei, 1983).

For diffusion not near the percolation threshold (where flux is discontinuous), accurate analytic solutions are possible by using the effective medium approximation (EMA) (Kirkpatrick, 1973). The modern version of the EMA was given by Kirkpatrick (1973), considering a randomly-distributed resistor network. A class of EMA's has been constructed by Sahimi et al. (1983), who also provided an excellent review of the theory. More recently, analytic solutions for diffusivities in bidisperse-pore media were derived from the EMA (Benzoni and Chang, 1984; Burganos and Sotirchos, 1987).

We first apply the EMA to one-dimensional diffusion in a zeolite with parallel pores (e.g., in mordenite), whose cation sites are occupied by n different cations, each with a fractional occupancy ϵ_i. The resulting equation is:

$$\frac{1}{D_m} = \sum_{i=1}^{n} \frac{\epsilon_i}{D_i} \tag{1}$$

where D_m is the mean (effective) diffusivity, and D_i is the diffusivity in zeolite containing 100% ith pores or cations of the ith kind.

We next consider diffusion in multidimensional (2D square or 3D simple cubic) zeolite networks. The self-consistency requirement from the EMA is (Kirkpatrick, 1973)

$$\int \frac{(k - k_m)}{k + \left(\frac{z}{2} - 1\right) k_m} f(k)\, dk = 0 \tag{2}$$

where z is the coordination number, k is mass conductance (or jump frequency), k_m is the mean value of k, and $f(k)$ is the probability distribution which is given by

$$f(k) = \sum_{i=1}^{n} \epsilon_i \delta(k - k_i) \tag{3}$$

where $\delta(k - k_i)$ is the Kronecker delta function.

By combining Eqs. 2 and 3, we have

$$\sum_{i=1}^{n} \frac{\epsilon_i (k_i - k_m)}{k_i + \left(\frac{z}{2} - 1\right) k_m} = 0 \tag{4}$$

The effective D_m is given by (via Einstein relation, $D = k\delta^2/2$):

$$\sum_{i=1}^{n} \frac{\epsilon_i (D_i - D_m)}{D_i + \left(\frac{z}{2} - 1\right) D_m} = 0 \tag{5}$$

Equation 5 is an nth polynomial equation for D_m. Regardless of the value of n, it can be shown that there is only one positive root for D_m which is the diffusivity in the zeolite containing n types of pore each having a diffusivity of D_i.

The solution for the binary system has been given by Kirkpatrick (1973). Thus, for a bidisperse-pore zeolite A or zeolite A containing two types of cation, the diffusivity is given by the quadratic form of Eq. 5 as (here $z = 6$ as shown in Figure 1 for A zeolite):

$$\frac{D_m}{D_1} = \frac{1}{4}[2 - 3\epsilon_2 + (3\epsilon_2 - 1)r] + \frac{1}{4}\{[2 - 3\epsilon_2 + (3\epsilon_2 - 1)r]^2 + 8r\}^{1/2} \tag{6}$$

where $r = D_2/D_1$. The limiting case for $r = 0$, in which pore type 2 is totally blocked, is

$$\frac{D_m}{D_1} = 1 - 1.5\epsilon_2 \; (= 1.5\epsilon_1 - 0.5) \qquad \epsilon_1 > \frac{1}{3} \tag{7}$$

Equation 6 is plotted in Figure 2 with r as the parameter. Numerical (Monte-Carlo) solutions for diffusivities in binary pore systems have been calculated by Ruthven (1974) and by Theodorou and Wei (1983). Ruthven's results are in excellent agreement with Eq. 6 and he also obtained Eq. 7 empirically (Figure 2). Theodorou and Wei considered a 2D square network with a probability of passing through an open pore = 0.25 and that through a blocked pore = 0.01. Thus, $r = 0.01/0.25 = 0.04$. Their numerical solution is in good agreement with the solution from Eq. 5 with $z = 4$.

Kinetic solutions for heterogeneous sites

The kinetic approach adopted here follows the classical transition state theory, which has been used previously to study diffusion in zeolites (Ruthven and Derrah, 1972; Riekert, 1971). As depicted in Figure 3, the passage of molecule A through the intercavity aperture may be considered as a rate process involving an activated transition state. Our consideration will be restricted to a binary-site zeolite, i.e., each cavity contains two types of adsorption sites, 1 and 2. Once activated, the molecule can take one of four possible paths. The rate constant for activation from site 1 is k_{a1}, and that for site 2 is k_{a2}. The rate constant for readsorption on all four sites should be the same and equal to the vibration frequency (ν) of the activated molecule. Thus, the

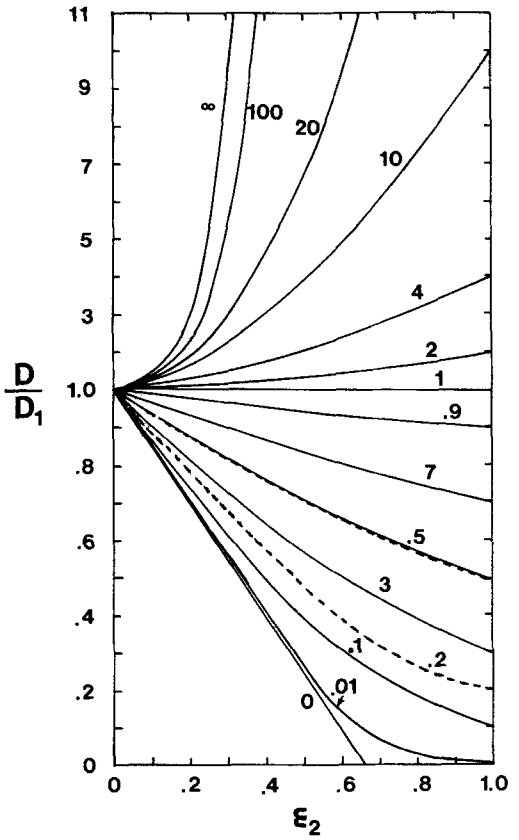

Figure 2. Analytic solution for pore blocking, Eq. 6, where $r(=D_2/D_1)$ is the parameter. ϵ_2 is fraction of K^+.

Also shown are Monte-Carlo calculation by Ruthven (1974) (dashed lines).

rates are:

Activation:

$$r_1 = k_{a1} C_{1,x-\delta/2} \tag{8}$$

$$r_2 = k_{a2} C_{2,x-\delta/2} \tag{9}$$

Readsorption:

$$r(\text{forward}) = \nu C^*_{x-\delta/2} (\theta_{v1} + \theta_{v2})_{x+\delta/2} \tag{10}$$

$$r(\text{reverse}) = \nu C^*_{x-\delta/2} (\theta_{v1} + \theta_{v2})_{x-\delta/2} \tag{11}$$

where θ_{v1} is the fraction of vacant type-1 sites, C_1 is the concentration of A adsorbed on type-1 sites, and $C^*_{x-\delta/2}$ is the concentration of the activated molecules originated from all sites at $x - \delta/2$.

The stationary state assumption stipulates that the change rate of the concentration of the activated species is zero, thus

$$\frac{dC^*_{x-\delta/2}}{dt} = k_{a1} C_{1,x-\delta/2} + k_{a2} C_{2,x-\delta/2} - \nu C^*_{x-\delta/2} [(\theta_{v1} + \theta_{v2})_{x+\delta/2} + (\theta_{v1} + \theta_{v2})_{x-\delta/2}] = 0 \tag{12}$$

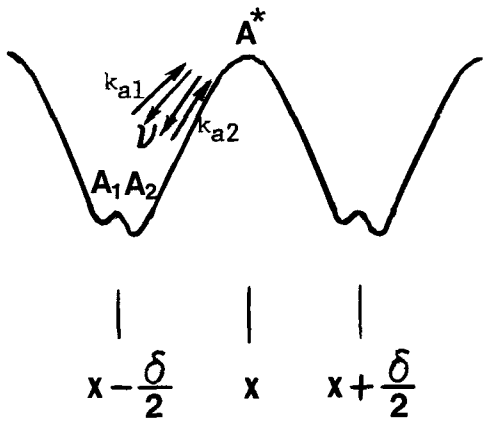

Figure 3. Potential energy diagram.

A_1 and A_2 are adsorbed A on sites 1 and 2, respectively. A^* is at activated state at an intercavity pore.

Equation 12 is solved for $C^*_{x-\delta/2}$. The same set of equations as Eqs. 8–12 are written for the activated molecule (located at x) originating from the cavity located at $x + \delta/2$, and they are solved for $C^*_{x+\delta/2}$.

The net forward mass fluxes for type-1 and type-2 sites are, respectively,

$$J_1 = \nu\delta(C^*_{x-\delta/2}\theta_{v1,x+\delta/2} - C^*_{x+\delta/2}\theta_{v1,x-\delta/2}) \tag{13}$$

$$J_2 = \nu\delta(C^*_{x-\delta/2}\theta_{v2,x+\delta/2} - C^*_{x+\delta/2}\theta_{v2,x-\delta/2}) \tag{14}$$

Substituting the solutions of C^* into Eqs. 13 and 14, noting $\theta_{v1} = \epsilon_1 - C_1/C_T$ (where C_T = total concentration of sites 1 and 2) and by carrying out the Taylor's series expansion (neglecting higher-order terms for infinitesimal δ), i.e.,

$$C_{x+\delta/2} = C_x + \frac{\delta}{2}\frac{\partial C}{\partial x} \tag{15}$$

we obtain

$$J_1 = -D_{11}\frac{\partial C_1}{\partial x} - D_{12}\frac{\partial C_2}{\partial x} \tag{16}$$

$$J_2 = -D_{21}\frac{\partial C_1}{\partial x} - D_{22}\frac{\partial C_2}{\partial x} \tag{17}$$

with the Fickian diffusivities:

$$D_{11} = \frac{\epsilon_1 D_{10} + \theta_2 D_{20}}{1 - \theta} \tag{18}$$

$$D_{12} = \frac{(\epsilon_1 - \theta_1) D_{20}}{1 - \theta} \tag{19}$$

$$D_{21} = \frac{(\epsilon_2 - \theta_2) D_{10}}{1 - \theta} \tag{20}$$

$$D_{22} = \frac{\epsilon_2 D_{20} + \theta_1 D_{10}}{1 - \theta} \tag{21}$$

where D_{10} and D_{20} are the intrinsic diffusivities, which are diffusivities at zero amount adsorbed, given by the Einstein relation:

$$D_{10} = \frac{k_{a1}\delta^2}{2}; \quad D_{20} = \frac{k_{a2}\delta^2}{2} \tag{22}$$

To simplify the above solutions for diffusivities, we assume that localized equilibrium is reached between molecules adsorbed on the two types of site with a partition constant K:

$$K = \frac{C_2}{C_1} = \frac{\theta_2}{\theta_1} \tag{23}$$

It follows

$$C_1 = \frac{C}{1+K}; \quad C_2 = \frac{KC}{1+K} \tag{24}$$

The total flux is obtained by summing Eqs. 16 and 17:

$$J = J_1 + J_2 = -\frac{D_{11} + D_{21} + K(D_{12} + D_{22})}{1+K}\frac{\partial C}{\partial x} \tag{25}$$

Substituting Eqs. 18–21 into Eq. 25, the overall diffusivity becomes:

$$D = \frac{D_{10} + KD_{20}}{1 + K - 2\theta} \tag{26}$$

Equation 26 provides the solution for the overall diffusivity, D, expressed in terms of the intrinsic diffusivities (i.e., diffusivities on sites 1 and 2 at $\theta = 0$). From Eq. 26, it is seen that D should increase as the surface coverage θ increases. For a zeolite containing only one type of cation, $D_{10} = D_{20} = D_o$ and $K = 1$, eq. 26 is reduced to:

$$D(\text{pure-cation}) = \frac{D_o}{1-\theta} \tag{27}$$

which is the same at the HIO model for surface diffusion (Yang et al., 1973). It is also the same, for no obvious reason, as the result for zeolitic diffusion based on Darken's relation for gases following the Langmuir isotherm (e.g., Yang, 1987, p. 120).

Equation 26 contains the partition constant K which remains to be evaluated. Evaluation of K is possible at low surface coverage. As the amount adsorbed approaches zero, from Eqs. 8–11 we obtain

$$k_{a1}C_1 = \nu C^*\epsilon_1; \quad k_{a2}C_2 = \nu C^*\epsilon_2 \tag{28}$$

and hence

$$K = \frac{C_2}{C_1} = \frac{k_{a1}}{k_{a2}}\frac{\epsilon_2}{\epsilon_1} = r\frac{\epsilon_2}{\epsilon_1} \tag{29}$$

Substituting Eq. 29 into Eq. 26 and letting $\theta = 0$, we have

$$\frac{D_o}{D_{10}} = \frac{r}{\epsilon_2 + r\epsilon_1} \tag{30}$$

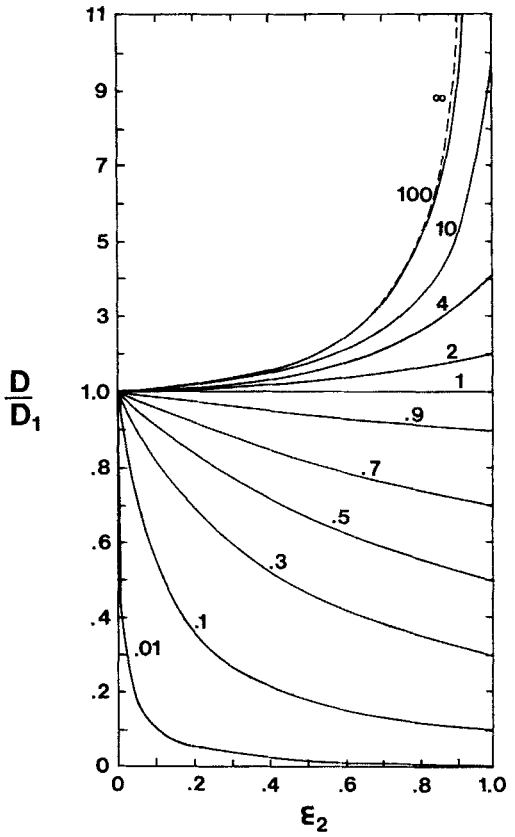

Figure 4. Kinetic solution for diffusivity (at $\theta = 0$) with heterogeneous sites in cavity at site-2 fraction ϵ_2 and parameter $r(=D_{20}/D_{10})$.

where $r = D_{20}/D_{10}$. The dependence of diffusivity on the amount of type-2 cations, ϵ_2, is shown in Figure 4 with r as the parameter.

Experimental

The diffusivities and equilibrium amounts adsorbed were measured by gravimetric uptake using a microbalance (TGA) which was connected to a gas flow system. Zeolite crystals in the powder form were used. The crystals were A-type molecular sieves containing pure or mixed cations of Na and K, ranging from 0–100% in composition. Details of the experimental technique and calculations are available elsewhere (Yeh, 1989). A summary is given below.

The zeolite sample was Na-A (4A) in powder form supplied by Linde Division of Union Carbide Corporation (Lot No. 94108606000 8A, MS-1071). Scanning electron microscope analysis showed that the crystals were nearly cubic in shape with a number-average size of 2.8 μm. The Na form was exchanged (partially or fully) for K^+ following the procedure published in the literature (Breck et al., 1956; Bolton, 1976). The ion exchange was performed at 25°C in 0.2N KCl solution in deionized water for an equilibration time of 3 days. Partial ion exchange was controlled by adjusting the initial K^+/Na^+ equivalent ratio, and the final K^+ concentrations of the exchange solutions were determined by the amounts of K^+ precipitated as $KClO_4$. The cation fractions in the samples prepared for this study were: $\epsilon_2 = K^+/(K^+ + Na^+) = 0$, 5%, 10%, 25%, 32%, 46%, 62%, and 100%.

Stringent steps were taken in the design, calibration and operation of the TGA/flow system in order to minimize or eliminate the undesirable factors which often plague the measurement of diffusivities in zeolite: nonisothermal effect, external resistance, and traces of moisture.

The TGA was a Cahn system 113 with programmed temperature control. Helium (>99.995% purity Linde) was used as the inert carrier gas and the gas for regeneration. The adsorptive gases were CH_4 (>99.0%, Linde), C_2H_6 (>99.0%, Linde), and CO_2 (>99.9%, Linde). Each gas passed through a separate presorber, each containing 18-g 5A zeolite pellets (at 25°C), before being mixed and entering the TGA system. These presorbers effectively removed all traces of moisture (as evidenced by no weight gain in control experiments) as well as other impurities. Prior to each diffusivity measurement, the presorbers were regenerated at 350°C (*ca.* 8 h) in He flow, cooled to 25°C, and were subsequently saturated (breakthrough) by the respective adsorptive gases. Gas compositions from the TGA were measured by GC. A minimum gas velocity of 2.5 cm/s was used to minimize or eliminate external mass transfer resistance and nonisothermal effects. The uptake rates did not increase beyond this flow rate.

In a typical experiment, the zeolite sample was 20 mg of crystals spread in a thin layer on the sample pan (alumina or quartz, *ca.* 1 cm in dia.). The sample was regenerated (350°C, 8 h) in He and cooled to 25°C or 50°C in He before the introduction of the adsorptive gas in the He flow. The concentration of the adsorptive gas was increased in a stepwise manner so that the isotherm and the diffusivities at various amounts adsorbed could be obtained. Corrections for the buoyancy and drag force caused by the step changes were made based on blank runs.

The uptake curves were fitted to a nonisothermal model (Yeh, 1989). The temperature rises were below 0.5°C. This was the combined result of using a small crystal size, small amounts of crystals, high gas flow rate, and stepped increases in concentration. To further ensure the isothermality of the experiments, desorption curves were obtained; in all cases, these curves were mirror images of the uptake curves. With the isothermality ensured, the evaluation of the diffusivities was based on the isothermal model, by numerical fitting using least squares. The numerical fitting program was implemented with an optimization algorithm (UVMIF subroutine) provided by IMSL.

Results and Discussion

Extensive experimental results were obtained for the equilibrium amounts adsorbed and diffusivities of three gases (CH_4, C_2H_6, and CO_2) in ion-exchanged zeolites ($\epsilon_2 = K^+$ fraction = 0–100%) at 25 and 50°C. The total pressure was 1 atm in all cases.

An understanding of the cation locations in the zeolite A structure is necessary before discussion of the experimental results. As shown in Figure 1, the cations are located at three different sites. There are a total of 23 sites in each unit cavity. Only 12 monovalent cations, however, are needed (to balance the 12 AlO_2 tetrahedrals in the unit). In the NaA zeolite, there are eight Na^+ located at site I, three Na^+ at site II, and one Na^+ at site III (Breck, 1974). The three cations at site II partially block the aperture (or pore) and influence the adsorption and diffusion. Hence the influence of these cations on diffusion could be interpreted by the pore-blocking theory described above, and their influence on adsorption could be explained by the "bond

Table 1. Equilibrium Adsorption and Diffusivity of C_2H_6 at 25°C in Zeolite A at Various ϵ_2, $\epsilon_2 = K^+/(K^+ + Na^+)$*

ϵ_2	P(kPa)	Q(g/g)	D(cm²/s)
0%	1.19	1.21×10^{-2}	9.60×10^{-13}
	28.5	6.13×10^{-2}	4.12×10^{-12}
	44.9	6.68×10^{-2}	4.90×10^{-12}
	65.6	7.09×10^{-2}	5.49×10^{-12}
	99.5	7.49×10^{-2}	6.07×10^{-12}
5%	1.18	1.23×10^{-2}	7.45×10^{-13}
	28.5	5.35×10^{-2}	1.76×10^{-12}
	44.6	5.97×10^{-2}	3.23×10^{-12}
	65.4	6.41×10^{-2}	3.53×10^{-12}
	99.9	6.74×10^{-2}	5.88×10^{-12}
10%	1.19	0.85×10^{-2}	4.90×10^{-13}
	28.5	4.41×10^{-2}	7.84×10^{-13}
	44.9	5.06×10^{-2}	1.76×10^{-12}
	65.3	5.78×10^{-2}	3.33×10^{-12}
	100.6	5.90×10^{-2}	3.72×10^{-12}
25%	1.19	1.5×10^{-3}	1.5×10^{-14}
	101.0	1.20×10^{-2}	7.8×10^{-14}
32%	100.6	0.0	0.0

*The results at 50°C are available in Yeh (1989).

Table 2. Equilibrium Adsorption and Diffusivity of CO_2 at 25°C in Zeolite A at Various ϵ_2, $\epsilon_2 = K^+/(K^+ + Na^+)$*

ϵ_2	P(kPa)	Q(g/g)	D(cm²/sec)
0%	0.588	6.07×10^{-2}	2.16×10^{-11}
	2.39	9.90×10^{-2}	3.53×10^{-11}
	9.65	13.3×10^{-2}	1.33×10^{-10}
	30.8	16.1×10^{-2}	1.53×10^{-10}
	100.8	18.0×10^{-2}	1.76×10^{-10}
5%	0.894	6.51×10^{-2}	1.57×10^{-11}
	4.89	10.8×10^{-2}	2.20×10^{-11}
	16.7	14.0×10^{-2}	7.64×10^{-11}
	60.1	16.7×10^{-2}	8.82×10^{-11}
	100.2	17.8×10^{-2}	1.49×10^{-10}
10%	0.893	5.74×10^{-2}	1.27×10^{-11}
	4.88	10.3×10^{-2}	2.16×10^{-11}
	16.7	13.7×10^{-2}	5.68×10^{-11}
	60.3	16.6×10^{-2}	9.60×10^{-11}
	100.4	17.4×10^{-2}	1.37×10^{-10}
25%	0.898	1.02×10^{-2}	1.9×10^{-14}
	4.79	6.07×10^{-2}	3.9×10^{-14}
	8.14	8.57×10^{-2}	5.9×10^{-14}
	13.4	11.3×10^{-2}	7.4×10^{-14}
	101.2	15.3×10^{-2}	1.8×10^{-13}
32%	0.839	9.0×10^{-3}	1.8×10^{-14}
	6.22	4.1×10^{-2}	1.8×10^{-14}
	19.9	9.8×10^{-2}	2.2×10^{-14}
	101.2	12.7×10^{-2}	2.6×10^{-14}
46%	0.701	6.0×10^{-3}	1.8×10^{-14}
	3.16	1.26×10^{-2}	1.8×10^{-14}
	19.3	7.60×10^{-2}	2.2×10^{-14}
	101.6	12.00×10^{-2}	3.3×10^{-14}
62%	4.66	1.2×10^{-3}	1.7×10^{-14}
	47.9	8.80×10^{-2}	1.7×10^{-14}
	101.0	10.1×10^{-2}	1.9×10^{-14}
100%	100.6	trace	—

*The results at 50°C are available in Yeh (1989).

percolation" theory (e.g., Kirkpatrick, 1973). The cations located at sites I and III are within the cavity; consequently, their influence on adsorption and diffusion is due to site heterogeneity.

The experimental results on equilibrium adsorption (Q) and diffusivity (D) for C_2H_6 and CO_2 in the mixed-cation zeolite A at 25°C are given respectively in Tables 1 and 2. Similar results for CH_4 at 25° and 50°C and that for C_2H_6 and CO_2 at 50°C are available in detail elsewhere (Yeh, 1989). The diffusivities increase with the amount adsorbed. The dependence of diffusivity on adsorbate concentration (Q) generally obeys Eq. 27, i.e., $D/D_o = (1 - \theta)^{-1}$ where $\theta = Q/Q_s$ (Yeh, 1989). Thus the diffusivities at zero coverage ($\theta = 0$) are obtained using Eq. 27, where the values of Q_s are calculated by fitting the equilibrium adsorption data with the Langmuir isotherm and the "monolayer" amount is taken as Q_s (Yeh, 1989).

In measuring the amounts adsorbed, true equilibria are difficult to achieve for zeolites with high K^+ contents due to low diffusivities. In the most severe cases, such as C_2H_6/25% K^+A at 25°C and CO_2/>46% K^+A at 25°C, 3–5 days were allowed for each measurement. The values for the equilibrium amounts adsorbed are thus pseudoequilibrium values. The main cause for low diffusivities is the proximity between the molecular size and the aperture size. The aperture sizes are 3.0 and 3.8 Å for KA and NaA, respectively, whereas the kinetic diameters (calculated from the Lennard-Jones potentials) are 3.3 and 3.8 Å for CO_2 and CH_4, respectively (C_2H_6 is slightly larger than CH_4). The kinetic diameter is an approximate value for the molecular size and thus provides an indication for the admission or exclusion to the zeolite cavities.

The experimental data on adsorption and diffusivity are also shown in Figures 5–10, for D_o (at $\theta = 0$) and Q (at 1 atm). Equilibrium adsorption data (but no diffusivity data) have been reported by Breck et al. (1956) for C_2H_6 and CO_2 in mixed Na/K type-A zeolite at 25°C and a fixed pressure of 0.921 atm (700 mm Hg). They reported values of approximately 0.072 g/g (at $\epsilon_2 = 0$) decreasing (convexing downward) to zero at $\epsilon_2 = 0.27$ for C_2H_6 (compared to the data in Figure 7 for 1 atm), and 0.18 g/g (at $\epsilon_2 = 0$) decreasing to 0.01 (at $\epsilon_2 = 0.95$) for CO_2 (compared to our data in Figure 9 for 1 atm). Their data are in good agreement with ours. The results shown in Figure 5–10 exhibit a general cut-off phenomenon at certain values of K^+ content (ϵ_2). An exception to the cut-off behavior is found in the amounts adsorbed of CO_2, where it declines with ϵ_2 to a finite value at

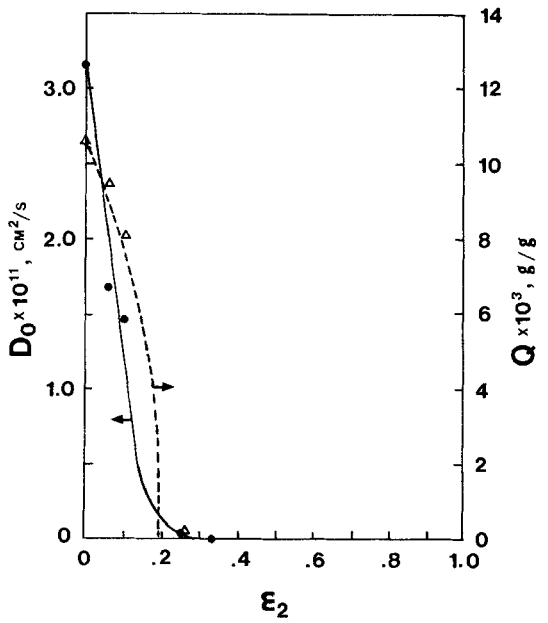

Figure 5. Equilibrium adsorption at 1 atm (Δ, Q).
Diffusivity at $\theta = 0$ (●, D_o) of CH_4 at 25°C in zeolite with K^+ fraction ϵ_2. Prediction by percolation theory for adsorption (dashed line) and that by pore-blocking theory for diffusivity (solid line).

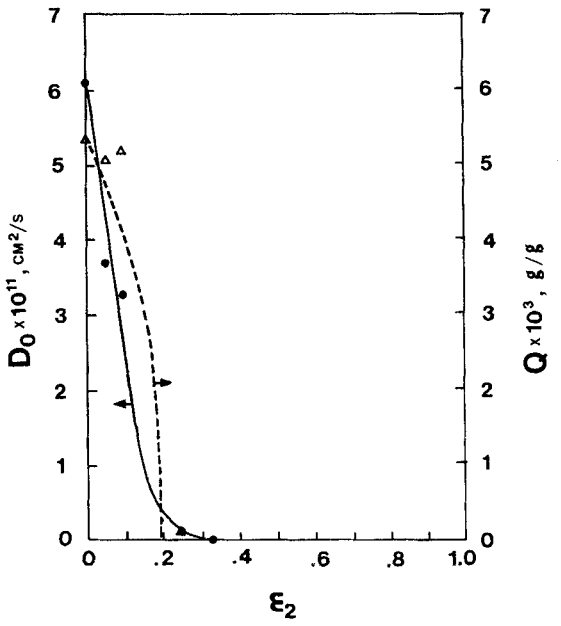

Figure 6. Equilibrium adsorption at 1 atm (Δ) and diffusivity at $\theta = 0$ (●) of CH_4 at 50°C in zeolite with K^+ fraction ϵ_2.
Prediction by percolation theory for adsorption (dahsed line) and that by pore-blocking theory for diffusivity (solid line).

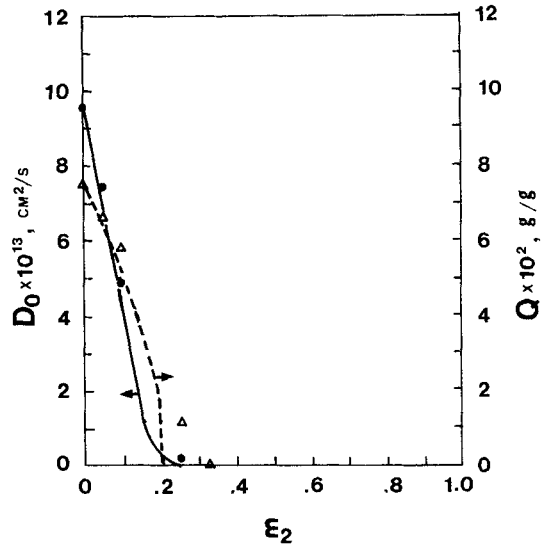

Figure 7. Equilibrium adsorption at 1 atm (Δ) and diffusivity at $\theta = 0$ (●) of C_2H_6 at 25°C in zeolite with K^+ fraction ϵ_2.
Dashed line, percolation theory for adsorption; solid line, pore-blocking theory for diffusivity.

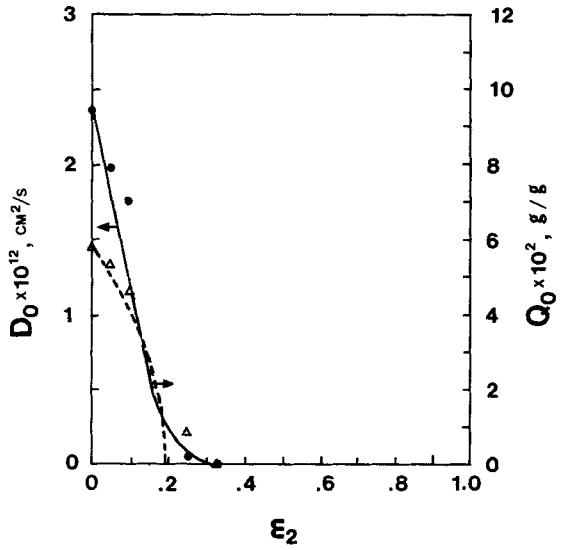

Figure 8. Equilibrium adsorption at 1 atm (Δ) and diffusivity at $\theta = 0$ (●) of C_2H_6 at 50°C in zeolite with K^+ fraction ϵ_2.

Dashed line, percolation theory for adsorption; solid line, pore-blocking theory for diffusivity.

100% K^+ (Figures 9 and 10). These values (at high ϵ_2) are however, kinetically-limited and are not near equilibrium. Specifically, the Q values for CO_2 at $\epsilon_2 = 46\%$ and 62% are higher at 50°C than those at 25°C. These values are clearly far from equilibrium and may be considered as "3-day" uptake amounts. The diffusivity data for CO_2, however, retain the cut-off behavior.

The cut-offs in the above results are also referred to as percolation thresholds (Kirkpatrick, 1973), which were first studied formally by Broadbent and Hammersley (1957). Percolation thresholds may be caused by bond (aperture) blocking or site (cavity) blocking. For the mixed-cation A zeolites, K^+ on sites I and III blocks neither aperture nor cavity, and hence is not

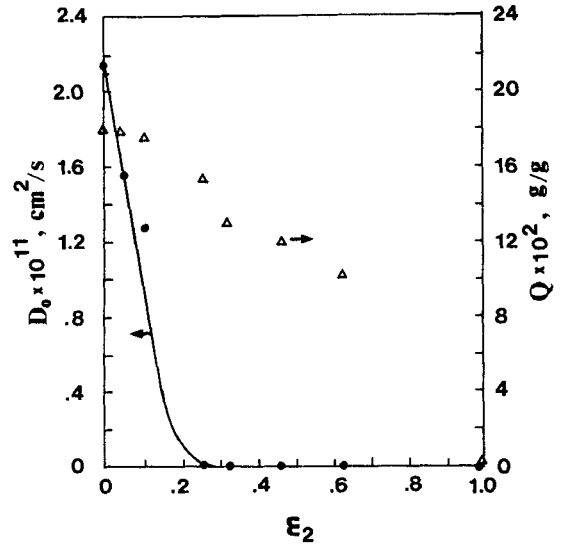

Figure 9. Equilibrium adsorption at 1 atm (Δ) and diffusivity at $\theta = 0$ (●) of CO_2 at 25°C in zeolite with K^+ fraction ϵ_2.

Solid line, pore-blocking theory for diffusivity.

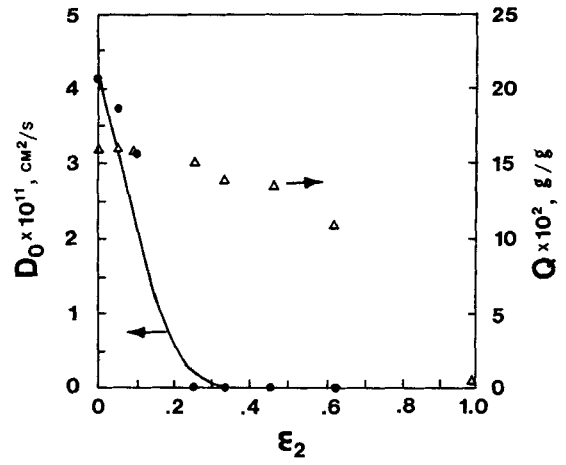

Figure 10. Equilibrium adsorption at 1 atm (Δ) and diffusivity at $\theta = 0$ (●) of CO_2 at 50°C in zeolite with K^+ fraction ϵ_2.

Solid line, pore-blocking theory for diffusivity.

responsible for the cut-off behavior. The cut-off behavior is therefore caused mainly by bond percolation. The zeolite type-A network (Figure 1) has a cubic structure. The result for bond percolation in a simple cubic system (Kirkpatrick, 1973) is shown in Figure 11. The theoretical percolation threshold is approximately 75% pore blockage.

The thresholds for the amounts adsorbed of CH_4 (Figures 5 and 6) and C_2H_6 (Figures 7 and 8) correspond to ϵ_2 values substantially lower than the theoretical value of 75%. A close inspection of the experimental results shows that the ϵ_2 values, where Q suddenly declines, are approximately ¼ of the theoretical threshold. As described above, there are three type-II sites for K^+ to displace Na^+, out of a total of 12 sites (eight on site I and one on site III). And these are the three sites where bond-blocking occurs. The experimental results of approximately ¼ of the theoretical threshold is a strong evidence to show that the three type-II sites are preferentially ion exchanged by K^+.

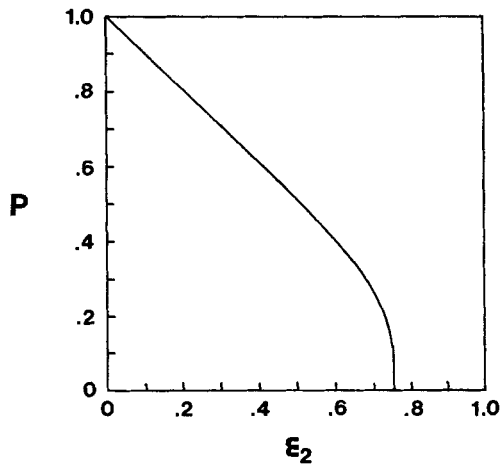

Figure 11. Fraction of accessible cavities (P) as a function of fraction of blocked pores (ϵ_2) from bond-percolation theory for 3D simple cubic lattice.

From Kirkpatrick (1973).

The aperture is totally blocked (for CH_4 and C_2H_6) when all three type-II sites are occupied by K^+. No information exists in the literature concerning the locations of the K^+ cations in the mixed K/Na zeolite.

Based on the preceding discussion, the amounts adsorbed for CH_4 and C_2H_6 are interpreted by bond percolation with a shifted threshold (or adjusted ϵ_2 values). The threshold is shifted from 75% to 1/4 of this theoretical value, i.e., 19%. The theoretical values for sorption capacities are thus plotted in dashed lines in Figures 5–8, which are in fair agreement with the experimental data. The bond percolation theory is applicable to CH_4 and C_2H_6 because the pores are closed (or bonds broken) when K^+ occupies site II. This is not the case for CO_2, however. Due to the small size of CO_2 (CO_2 is a linear molecule), pores are not closed to CO_2 with K^+ occupying site II. Consequently, the equilibrium amount of adsorbed CO_2 declines relatively slowly with % K^+ exchange, as shown in Figures 9 and 10, and the CO_2 data do not exhibit a percolation threshold.

It has become clear that pore blocking plays a major role in both sorption capacity and diffusivity in the systems studied here, while site heterogeneity plays only a secondary role. The analytic solution for pore blocking based on EMA will be used to interprete the diffusivity data. In applying the pore-blocking solution, the value of ϵ_2 (i.e., extent of K^+ exchange) needs to be adjusted to that consistent with the theory. Since the three site-II cations are preferentially exchanged (out of a total of 12 cations), the effective ϵ_2 value should span from 0 to 25% (3/12) of the actual K^+ fractions. With this adjustment, the EMA/pore-blocking theory is applied by using Eq. 6. Moreover, the limiting diffusivities, D_1 and D_2, are the values corresponding to $\epsilon_2 = 0$ and 25%, respectively. The values of r used in predicting D_m are D_{20}/D_{10}, where D_{20} is D_o at $\epsilon_2 = 25\%$ and D_{10} is D_o at $\epsilon_2 = 0$. The values of D_o are obtained from the diffusivity data using Eq. 27, where $\theta = Q/Q_s$ and Q_s is calculated from the Langmuir isotherm (Yeh, 1989). Thus, there are no fitting parameters used in the prediction. The predicted diffusivity (D_m) values calculated from Eq. 6 are also shown in Figures 5–10 as solid curves. The pore-blocking theory provides a fair interpretation for the experimental values in the ϵ_2 range of 0–25%.

As the K^+ content exceeds 25%, the K^+ cations start to occupy types I and III sites. The variation of diffusivity is dominated by site heterogeneity. The theoretical solution, Eq. 30, should be applicable in this region. To do so, the limiting diffusivities at $\epsilon_2 = 25\%$ (for D_1) and 100% (for D_2) are required. However, measurement of diffusivity in this region (especially at $\epsilon_2 = 100\%$) is not feasible with the TGA (or any other existing) technique due to the small amount adsorbed and the low diffusivity. Consequently, the value for r in Eq. 30 ($r = D_2/D_1$), although it is known to be small, cannot be evaluated. The theoretical solution (Figure 4) predicts a sharp decline of diffusivity for small values of r, which is qualitatively in agreement with the experimental results.

Acknowledgment

We thank Professor Stratis Sotirchos of the University of Rochester for a helpful discussion on EMA. We are indebted to the Donors to the Petroleum Research Fund administered by the American Chemical Society for their support.

Notation

C = concentration (or total concentration) of adsorbed molecules
C_1, C_2 = concentration of adsorbed molecules on site 1 or 2
D = diffusivity
D_{10}, D_{20} = intrinsic diffusivity on site 1 or 2 defined by Eq. 22, or diffusivity at zero coverage
J = flux or molecules
k = mass conductance or jump frequency
k_a = rate constant for activation
K = equilibrium partition constant between two types of site
P = pressure
Q = equilibrium amount adsorbed
r = D_2/D_1 or D_{20}/D_{10} or rate
t = time
x = distance coordinate
z = coordination number (number of pores connected to each cavity)

Greek letters

δ = jump distance or intercavity distance
ϵ_i = fraction of pores of the ith kind, or fraction of cation sites occupied by cations of the ith kind
ϵ_2 = K^+ fraction, $K^+/(K^+ + Na^+)$
θ = fractional coverage of adsorption sites
θ_v = fractional vacant sites
ν = vibration frequency

Subscripts

i = related to ith pores or ith cations (1 for Na^+, 2 for K^+)
m = mean value
s = saturated
0 = properties at zero surface coverage
1, 2 = adsorption sites 1 and 2

Literature Cited

Barrer, R. M., *Zeolites and Clay Minerals*, Academic Press, New York, (1978).

Benzoni, J., and H. C. Chang, "Effective Diffusion in Bidisperse Media—An Effective Medium Approach," *Chem. Eng. Sci.*, **39**, 161 (1984).

Bolton, A. P., "Molecular Sieve Zeolites," *Expt. Methods in Catal. Res.*, **II**, 1 (1976).

Breck, D. W., *Zeolite Molecular Sievens*, Wiley, New York (1974).

Breck, D. W., W. G. Eversole, R. M. Milton, T. B. Reed, and T. L. Thomas, "Crystallization Zeolites: I. The Properties of a New Synthetic Zeolite, Type A," *J. Am. Chem. Soc.*, **78**, 5963 (1956).

Broadbent, S. R., and J. M. Hammersley, "Percolation Processes: I. Crystals and Mazes," *Proc. Camb. Philos. Soc.*, **53**, 629 (1957).

Burganos, V. N., and S. V. Sotirchos, "Diffusion in Pore Networks: Effective Medium Theory and Smooth Field Approximation," *AIChE J.*, **33**, 1678 (1987).

Gavalas, G. R., and S. Kim, "Periodic Capillary Models of Diffusion in Porous Solids," *Chem. Eng. Sci.*, **36**, 1111 (1981).

Kirkpatrick, S., "Percolation and Conduction," *Rev. Mod. Phys.*, **45**, 574 (1973).

Mo, W. T., and J. Wei, "Effective Diffusivity in Partially Blocked Zeolite," *Chem. Eng. Sci.*, **41**, 703 (1986).

Riekert, L., "Rates of Sorption and Diffusion of Hydrocarbons in Zeolites," *AIChE J.*, **17**, 446 (1971).

Ruthven, D. M., "Diffusion in Partially Ion Exchanged Molecular Sieves," *Can. J. Chem.*, **52**, 3523 (1974).

Ruthven, D. M., and R. I. Derrah, "Transition State Theory of Zeolitic Diffusion," *J. Chem. Soc. Farad. I*, **68**, 2332 (1972).

Sahimi, M., B. D. Hughes, L. E. Scriven, and H. T. Davis, "Stochastic Transport in Disordered Systems," *J. Chem. Phys.*, **78**, 6849 (1983).

Sahimi, M., and T. T. Tsotsis, "A Percolation Model of Catalyst Deactivation by Site Coverage and Pore Blockage," *J. Cat.*, **96**, 552 (1985).

Theodorou, D., and J. Wei, "Diffusion and Reaction in Blocked and High Occupancy Zeolite Catalysts," *J. Cat.*, **83**, 205 (1983).

Yang, R. T., *Gas Separation by Adsorption Processes*, Butterworth, Boston (1987).

Yang, R. T., J. B. Fenn, and G. L. Haller, "Modification of the HIO Model for Surface Diffusion," *AIChE J.*, **19**, 1052 (1973).

Yeh, Y. T., "Diffusion and Adsorption of Gases in Molecular Sieves," PhD Diss., SUNY at Buffalo (1989).

Manuscript received May 30, 1989, and revision received Aug. 4, 1989.